Nanostructure of Potato Starch. II. Structure of a Highly Crystalline Gel Obtained by Retrogradation Using X-Ray Diffraction Techniques

R. K. Bayer,* F. J. Baltá-Calleja

Instituto de Estructura de la Materia, CSIC, Serrano 119, 28006 Madrid, Spain

Received 31 January 2006; accepted 17 March 2006
DOI 10.1002/app.24527
Published online in Wiley InterScience (www.interscience.wiley.com).

ABSTRACT: A highly crystalline gel (65% crystal portions) was prepared by retrogradation of injection-molded potato starch in humid atmosphere. The different components of the nanostructure were identified by means of successive melting processes using "*in situ*" simultaneous wide and low angle X-ray diffractions. At low temperatures, structural changes such as annealing phenomena or evaporation of water, giving rise to a thickening of the gel, are observed. In the range of 55–75°C, a first transition due to melting of a layered structure of concentric sphere-like alternating crystalline and amorphous lamellar shells (amylopectine, AP, being the crystalline component) is detected. Analysis of results reveals that the AP crystallization contributes 25% to the overall crystal fraction. A spherulitic structure of alternating radial lamellae from amylose (AM) or AP melts in a higher temperature region between 75 and 86°C. This modification represents the major contribution to crystallinity of about 40%. Unexpectedly, the crystalline blocks of such a structure are abnormally anisometric; i.e., they are thicker than their width. This has been related to a contraction of the AMAP-co-spherulite due to an excessive growth of the AP-shell crystals. The anisometry of the blocks of the AMAP lamellae vanishes at the beginning of the melting of the AP shell crystals, just when the total crystallinity decreases below 50% at 60°C. © 2007 Wiley Periodicals, Inc. J Appl Polym Sci 104: 689–696, 2007

Key words: amorphous starch; WAXS; SAXS; retrogradation; nanostructure

INTRODUCTION

In a preceding study (Part I), the first stages of crystallization in amorphous potato starch initiated by diffusion of water were investigated.[1] It was established that amylose (AM) is the component that crystallizes first, its lamellae building up spherulites.[2] According to previous results,[3] AM in the molten state interpenetrates into the free space within the branches of the amylopectine (AP) molecules. It appears that densely ramified zones of the AP are not well accessible by other molecules.[4] Hence, whether an AM network may develop or not into its area strongly depends on the molecular architecture of the AP molecule. The less densely ramified AP molecules might have a better ability to crystallize. Furthermore, the AM within the AP will form radial crystalline lamella originating from the center of the AP molecule. The AM lamellae nucleate the crystallizable regions of the AP molecule to form radial lamellae too, being inserted into the interspaces between the AM crystals. The AP molecules, well interpenetrated by the AM, represent a system especially capable to form an AMAP-co-spherulite. The crystallized AMAP zones cover about 60% of the volume of potato starch. The remaining 40% of the volume consists of less perfect, AM-free AP molecules.[3] Because of the longtime storage in humid atmosphere, these molecules too are stimulated to crystallization.

The aim of the present study is to analyze the emerging complex crystalline structure from the different components arising through the successive melting processes, by means of simultaneous wide angle (WAXS) and small angle X-ray scattering (SAXS) measurements.

EXPERIMENTAL

Materials and heat treatment

Potato- and pea-starch samples were processed (employing an ARBURG-Allrounder 250S) using the elongational-flow injection-molding method.[5,6] This technique yields ductile, oriented amorphous starch materials.[7] A melt temperature of 140°C and a molding

**Present address:* Universität Gesamthochschule Kassel, Mönchebergstr.3, D-34125 Kassel, Germany.
Correspondence to: R. K. Bayer (rbayer@uni-kassel.de).
Contract grant sponsor: MEC, Spain; Contract grant number: FIS2004–01331. Contract grant sponsor: IHP-Contract, European Community; Contract grant number: HPRI-CT-1999–00040

temperature of 25°C were used. The molded samples were kept at ambient atmosphere, i.e., a humidity of 12%, and 1-mm cuts were prepared. The samples were investigated "*in situ* " by WAXS as follows. Injection-molded potato starch was held for 20 days in a moist atmosphere, which gave rise to a 65% crystallinity.[8] The samples were successively molten by gradually increasing temperature at the rate of 10°C/min. Particularly, the temperature region short before the complete disappearance of the crystals is of special interest.

Techniques

SAXS and WAXS were performed using a double-focusing camera adapted for the synchrotron radiation source at the polymer beamline A2 of HASYLAB, DESY, Hamburg. The wavelength used was 0.15 nm with a band pass of $dl/I = 5 \times 10^{-5}$. Scattering patterns were recorded every 30 s using a linear position-sensitive detector. The patterns were corrected for fluctuations in intensity of the primary beam and for the background. The accumulation time per frame was 30 s. The integral breadth of the reflections $d\beta$ was directly measured from the experimental profile to make an estimate of the value for the coherently diffracting domains $t \sim 1/d\beta$, normal to the chain direction as a function of temperature. The long period L has been derived from the SAXS measurements.

The major results of this study have been reported previously.[8] In the present investigation, additional evaluations of the linear crystallinity ($X_{cL} = t/L$), the fraction of crystallized lamellar stacks within the amorphous surroundings, $X_S X_L$, and the electron density difference, $\Delta\rho'^2$ between crystalline and amorphous phase, related to the sample volume, are presented.[1]

RESULTS

Selective melting of the different crystalline components

After 20 days storage time in humid atmosphere, the initially amorphous sample has reached a level of 65% crystallinity. Hence, one may assume that not only the spherulitic cocrystallization of AM and AP contributes to the total crystallinity, but also the single AP molecule semicrystalline superstructure of spherical shells, too.[9] A partial melting process thus should begin with the single AP molecule of the semicrystalline superstructure, a second melting step is supposed to include the AP of the AMAP-co-spherulite. Finally, close to the maximum melting temperature, the pure AM crystallites that are built up first should disappear.

Figure 1 exhibits three melting regions: (1) Up to 55°C, no considerable melting occurs, (2) from 55 up to 75°C, a melting of 25% of the overall crystal fraction takes place, and (3) the remaining 40% of crystals comparatively sharply melt in a temperature range of about 10°C. It seems reasonable to attribute the broad melting process occurring at low temperatures to the AP supercrystalline spherical structure which was formed last. Consequently, the AMAP spherulites are more temperature stable. The melting process ends in a still sharper step, corresponding to the fusion of pure AM crystals (~15% crystallinity, Fig. 1).

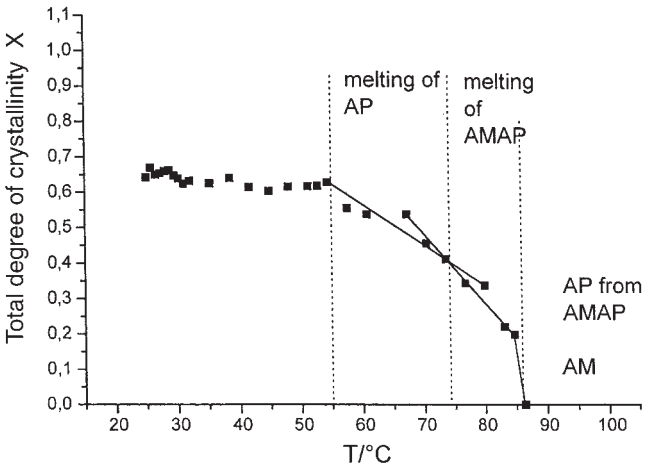

Figure 1 Total crystallinity, X_c, of initially amorphous potato starch, 20 days retrograded in humid atmosphere during successive melting processes. Heating rate: 10°C/min.

The above interpretation is supported by an estimation of the volume fraction of the respective crystal species:

$$V_i = \Delta X_i / \Delta X_T \quad (1)$$

where ΔX_i is the volume fraction of crystals of the i species and ΔX_T is the total initial crystallinity. This yields for V_{AP} = 25%/65% = 38.5%, and consequently, for V_{AMAP} = 40%/65% = 61.5%, in good agreement with the respective reported values given in Part I.[1] The volume fraction of pure AM crystals (15%/65% = 23%) from Figure 1 results as a meaningful estimation of the AM fraction of potato starch.

Nanostructure variation during thermal treatment: Characteristic regions

Figure 2 comparatively illustrates the variation of the total degree of crystallinity, X_c, in contrast with that of the linear crystallinity, $X_{cL} = t/L$, and the fraction of crystallized lamellar stacks, $X_S X_L = X_c/X_{cL}$, as a function of temperature.

Four temperature regions (A, B, C, D) can be distinguished. In range A (25–45°C), the total crystallinity decreases only slightly. In range B (45–55°C), the crystalline fraction slightly increases. Range D denotes the

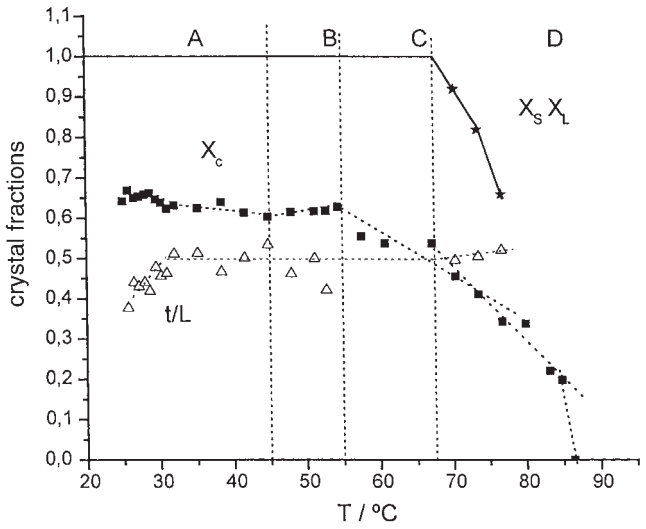

Figure 2 Crystal fractions X_c, t/L, and $X_S X_L$ as functions of temperature.

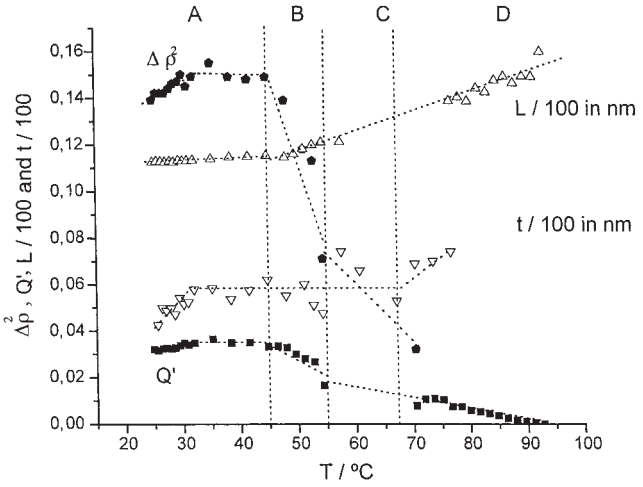

Figure 3 Invariant Q′ and $\Delta\rho'^2$ from SAXS, and long period L and crystal width t values as a function of temperature. Potato starch crystallized 20 days in humid atmosphere.

sharp drop of $X_S X_L$ below 1 (at ~67°C). The quantity t/L reaches the value of X_c at the end of region C. In case of $X_c > 50\%$, t/L should agree with the linear crystallinity of X_{cL}, up to the end of range C. However, the quantity t/L is always smaller than X_c. This means that within the ranges A–C, the mean width t of the crystal blocks is always smaller than the thickness l_c of the crystal lamellae consisting of mosaic blocks. Hence, Wulff's law, $t \approx l_c$, does not hold any more for highly crystalline potato starch. $X_S X_L$ cannot, therefore, be calculated from t/L. The condition $X_{cL} = X_c$ necessary for $X_c > 0.5$ leads, however, to $X_S X_L = 1$ within the whole region A–C. Above 67°C (range D), both the anisometry of the crystal blocks (t/L reaches the value of X_c here), as well as the percolation of the crystals vanish ($X_S X_L < 1$, $X_c < 0.5$).

Figure 3 illustrates the variations of the long period L, the invariant Q' of SAXS, and $\Delta\rho'^2$, derived from Q', as a function of temperature. Figure 4 shows the changes of crystallinity for the isolated AP molecules. In Figures 3 and 4, the temperature ranges A–D are particularly well recognized.

Analysis of nanostructural parameters

To further analyze the nature of the transitions, a separation of the influence of the different crystalline components on the long period is attempted below. Figure 5 shows a summary of L and t data, including results from Ref. [1]. The data of Ref. [1] refer to the temperature region (below 70°C) where AP molecular crystals are capable to crystallize.

In the region of $X_c = 0.2$–0.4 (see Fig. 1), the results for the AMAP spherulites overlap for both series, fitting well to a straight line which may be extrapolated into the range of higher crystallinities. Here the crystallinity data of the A and B range are also presented. Because of the influence of the AP sphere shell crystalline superstructure on the average values of L and t, a deviation from the extrapolated straight line at lower X_c values is observed (see Fig. 5). As L_{AMAP} (X_c) is known from Figure 5, L_{AP} (X_c) can be calculated from that difference.

The equation

$$L = V_{AMAP} L_{AMAP} + V_{AP} L_{AP} \qquad (2)$$

averages the long periods of both crystal types corresponding to the respective volume fractions (see eq. (1)). Figure 6 shows as well the measured $L(T)$, the

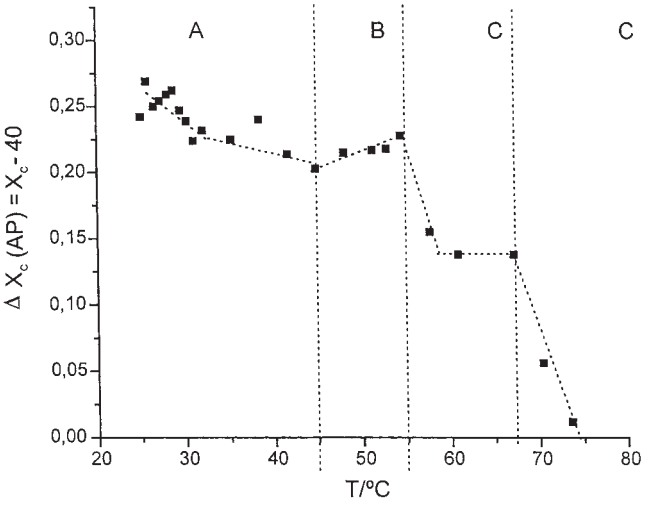

Figure 4 Partial melting of the crystal fraction which corresponds to isolated AP molecules.

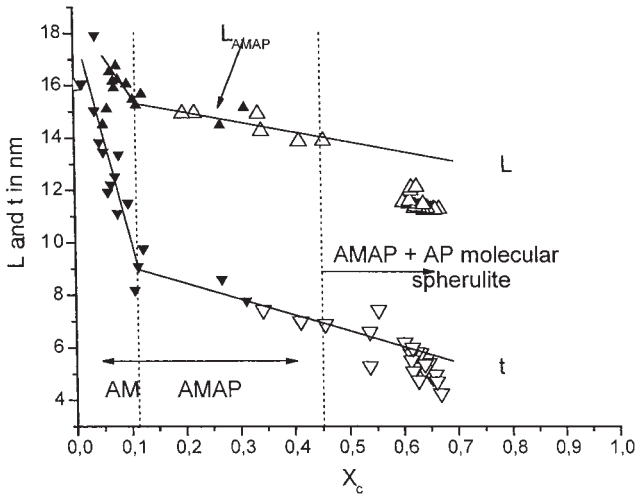

Figure 5 Plot of long period, L, and crystal block width, t, as a function of total degree of crystallinity, X_c. Data for the early stage of retrogradation[1]: filled triangles, data of the present article: open triangles. Maximum temperature: 70°C.

extrapolated $L_{AMAP}(T)$, and $L_{AP}(T)$ values calculated from eq. (2).

In the temperature range A (up to 45°C), L_{AP} is ~8 nm, in good agreement with the long period of native AP grains with a shell-like structure. The 8 nm value has also been observed from the early retrogradation of amorphous AP (Waxy Maize[9]). The result is plausible, as isolated AP molecules, which are not penetrated by the AM network,[3] should not crystallize in a manner different from pure AP. In both cases, the AP forms a large molecular spherulite, with the shape of a grain. The structural changes in range B must include a partial melting of imperfect shell crystal layers of the AP molecule: L_{AP} exhibits for pure AP, as pointed out previously,[9] a fast increase with temperature short before the shell structure disappears and melts when the long period reaches an end value of 15 nm. The bend in Figure 6 could hence be explained by a gradual melting of interlayers of sphere shell crystalline lamellae.

For $X_c > 0.5$, the thicknesses of the crystalline and amorphous layers of both crystal types can be calculated as well. In this case, $X_{cL} = X_c^*$, where X_c^* means that the crystal fraction X_c is related to the respective AMAP or AP fraction.

For free AP:

$$X^*_{AP} = (X_c - 0.4)/V_{AP} \tag{3}$$

$$V_{AP} = (X_c - 0.4)/X_c$$

where:

which leads to:

$$X^*_{AP} = X_c \tag{4}$$

Similarly one can derive:

$$X^*_{AMAP} = X_c \tag{5}$$

Equations (4) and (5) are valid as far as X_c^* (AMAP) and X_c^* (AP) are larger than 0.5, i.e., eq. (4) holds for $X_c > 0.52$ and eq. (5) for $X_c > 0.2$. Then one can determine the crystal thickness $l_{c\ AP}$ as:

$$l_{cAP} = X_c L_{AP} \tag{6}$$

and similarly:

$$l_{cAMAP} = X_c L_{AMAP} \tag{7}$$

Figure 7 shows the above quantities and the thickness of the amorphous layers $l_a = L - l_c$ as a function of temperature.

The shell crystals of the AP molecule are ~5 nm thick. According to Vandeputte et al.,[10] the outer bundles of an AP molecule can only form stable crystals, if they have a length of 12–22 monomers. A shell thickness of 5 nm corresponds to 5 nm/0.425 nm = 12 monomers.

The shell crystals of free AP molecules that fill ~38% of the volume of the crystallized potato starch are, therefore, close to the minimum of thermodynamic stability of the AP crystals. One can, therefore, assume that the better crystallizing AP molecules are already included into the nucleation by amylose crystals (AMAP). From Figure 7, one observes that $l_{c\ AMAP}$ practically does not vary with temperature, showing a value of ~8.5 nm. This average value corresponds to 20 starch monomers associated to better crystallizing AP molecules which obviously interact with the linear

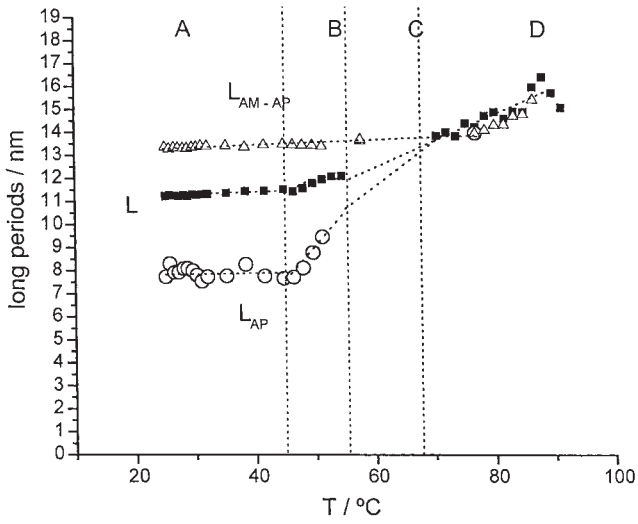

Figure 6 Experimental values of long period, L, L_{AMAP}, (extrapolated from Fig. 5), and of L_{AP} (calculated from eq. (2)) as a function of temperature.

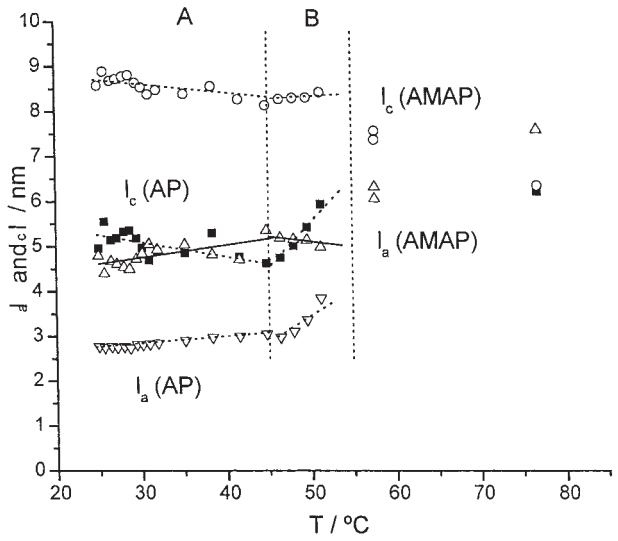

Figure 7 Crystalline and amorphous thicknesses of the AMAP spherulites and AP semicrystalline superstructure from potato starch, calculated from eqs. (6) and (7) and data from Figure 6.

AM chain segments. It is also noteworthy that the value of $l_{c\ AP}$ is very close to the width t of the crystal blocks through the whole temperature range (Fig. 8).

A possible explanation could be that the experimental t value (Fig. 3) does not represent an average of different t values of the two types of crystal nanostructure, but that it is the same for both. This would imply that the crystal blocks in the AP-shell-crystals are isometric, as proposed previously by us for pure AP.[9] Furthermore, this results suggests that the mean anisometry of the crystal blocks (as seen from Fig. 2 by $t/L < X_{cL}$) has to be attributed only to the AMAP-cospherulites. Figure 7 shows that the crystal thickness l_c

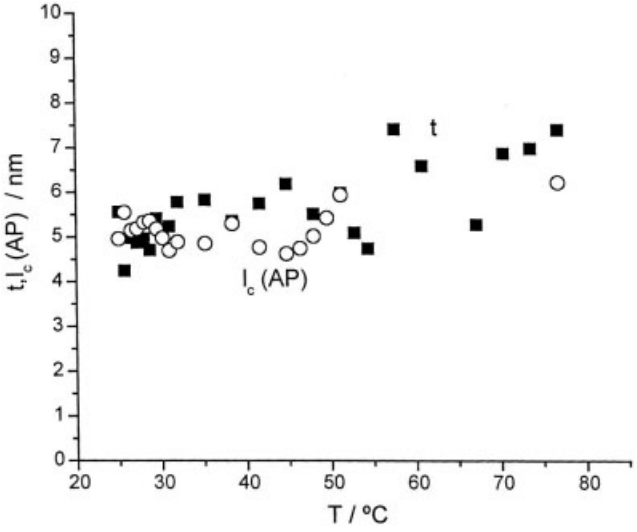

Figure 8 Comparison of $l_{c\ AP}$ and t values (from Figs. 7 and 3).

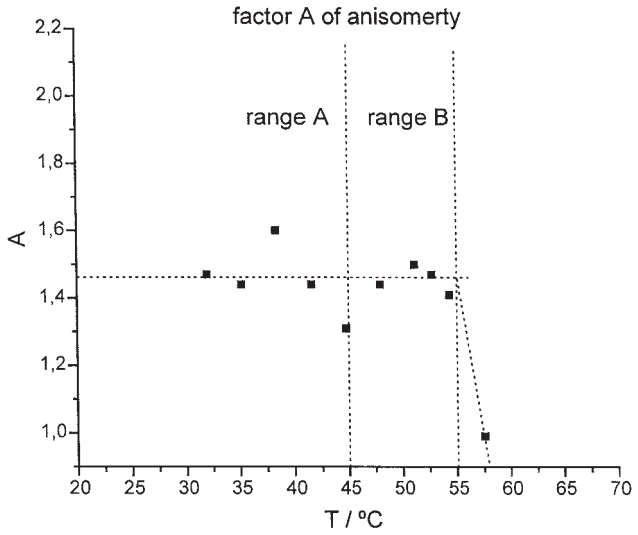

Figure 9 Plot of anisometry factor, A, (eq. (8)) as a function of temperature.

$_{AMAP}$ is ~8.5 nm, while the value t (Fig. 8) is only about 5 nm. The lateral dimensions of the crystal blocks within the AMAP morphology is determined by the width of the outer bundles of the AP molecule. Figure 5 shows that t = 5 nm corresponds to a value for highly developed crystallization typical for AP.[9] Figure 5 also shows that at the end the crystal formation by AM alone, t = 8.5 nm. In this case, owing to the low crystallinity (X_c = 12%), the AM crystal blocks should be isometric, i.e., $l_{c\ AM}$ = 8.5 nm. Obviously, this crystal thickness value predetermines the thickness of the crystals during the following AMAP crystallization.

In summary, the AMAP crystalline phase can be characterized as follows. The formation of a spherulite is controlled by the straight radial lamella, whose crystalline blocks have the width of the AP outer bundles and the thickness of the preexisting AM crystal blocks.

Let us define an anisometry factor as:

$$A = l_{c\mathrm{AMAP}}/t \tag{8}$$

The value of A calculated from the data of Figures 3 and 7 is shown as a function of temperature in Figure 9.

From Figure 9, it is seen that A_{AMAP} does not vary in the temperature ranges A and B (up to 55°C). This result fits well with the fact that all changes in this temperature region are due to modifications of the structure of AP crystals, but not due to an alteration of the temperature-stable AMAP crystallization.

DISCUSSION OF RESULTS

From the structural results obtained, we wish next to explain more in detail the structural transitions ob-

served through the various temperature ranges (A–D) studied.

Temperature range A (25–45°C)

In region A, despite the low temperatures involved, slight, but however, significant partial melting takes place. The total degree of crystallinity X_c is shown to decrease from 66 to 61% (Fig. 2). Simultaneously $l_{c\ AP}$ decreases as well (Fig. 7). Unexpectedly, the thicker crystals are the first ones to melt. However, in a preceding study, it was shown that this behavior is typical for the grain-shaped AP shell crystalline superstructure.[9] The thicker crystals are, indeed, the first ones that melt, because thickness growth is interconnected with strong inner tensions of the branched amorphous interlayers.

Another peculiarity appears at the beginning of range A, in the temperature interval from 25–32°C: the width of the crystal blocks, t, increases from 4.3 to 5.8 nm (Fig. 3). According to Vandeputte et al.,[10] the small crystal blocks (4.3 nm thick according to 10 monomers, assuming isometry) are not stable anymore. This could explain the early melting of these crystals. Figure 3 also shows that for this initial temperature region $\Delta\rho'^2$ increases up to a constant value, which does not change anymore up to the end of region A. Any influence of the electron density ρ_a of the amorphous phase on $\Delta\rho'^2 = (\rho_c - \rho_a)$ has to be excluded, as this should lead to a decrease, as observed in region B. The increase of $\Delta\rho'^2$, thus, must be due to an increase of ρ_c, perhaps due to an improvement in the perfection of the crystals. This can be easily concluded from the partial melting of the smaller crystallites in that temperature interval. This is the reason why this temperature region has not been considered for the calculation of the AMAP crystal blocks (Fig. 9). The AP molecules incorporated into the AMAP semicrystalline superstructure were regarded as the better crystallizing ones. Therefore, it is not meaningful to attribute the immediate melting of imperfect crystals from the AP sphere shell crystal organization to the temperature-stable AMAP spherulites. Consequently, the low t values at the beginning of the temperature program have not been included into the evaluation of the anisometry factors (Fig. 9). This curve does not start below 32°C.

Temperature range B (45–55°C)

Figure 3 bears the key understanding of region B. The quantity $\Delta\rho'^2$ does not appreciably change in the high X_c range (especially in the region 32–45°C), i.e., neither the density of the amorphous nor that of the crystallites varies. However, in region B ($X_c \leq 0.63$) $\Delta\rho'^2$ strongly decreases. From other experiments,[11] one can assume that due to the high moisture content of the potato starch gel, the density of the amorphous phase must be notably lower than that of the crystalline one. After finishing the time-temperature-program and returning to room temperature, the observed pearls of condensed water inside the glass capillary sweat out of the gel. Hence, the decrease of water concentration could explain the decrease of $\Delta\rho'^2$ in range B. As a result, ρ_a would increase and finally approximate to ρ_c, giving rise to the drop of $\Delta\rho'^2$ in region B, despite the slight crystallinity increase. Hence, the swollen grains of the semicrystalline structure of AP should shrink in region B, leading to a complete reorganization of the AP molecule crystal, as indicated by the parallel increase of long period (Fig. 6), of crystal thickness $l_{c\ AP}$ (Fig. 7), and crystallinity $\Delta X_{c\ AP}$ (Fig. 4). The defect structures of the AP molecule vanish during the thickening process of the gel, leading to an improvement of crystal perfection. While the AP crystal structure experiences modifications in range B, the AMAP spherulites are practically unaltered. As a consequence, $l_{c\ AMAP}$, (Fig. 7), L_{AMAP} (Fig. 6), and the anisometry of the crystal blocks (Fig. 9) hardly change.

Temperature range C (55–67°C)

Region C denotes the end of the AP shell structure. At 58°C, the crystallinity $X_{c\ AP}$ is still at 12.5% (Fig. 4), which corresponds to half of its initial contribution $X^*_{AP} = 50\%$. Furthermore, the secondary network outside the AP molecules loses its stabilizing effect. Some particular, weak crystalline superstructures may already collapse leaving an unorganized zone from crystal blocks of a relative crystallinity, $X^*_{c\ AP}$, of 20%.zref9 The AMAP phase is not much influenced in range C, as shown by the constancy of L_{AMAP}. The occurrence of some lateral freedom (due to the disappearance of some AP supercrystals) (Fig. 6), however, induces an anisometry decrease of its crystal blocks, down to $A = 1$ (see Fig. 9). The crossover of the t/L curve with the $X_c(T)$ curve near 50% (Fig. 2) may be interpreted in the same sense. Because of the minimization of surface to volume ratio, the anisometry of the AMAP crystal-blocks is not favored thermodynamically. Owing to the loss of percolation of the AP super crystals, lateral freedom originates, and energetic reasons should not exist anymore to maintain the anisometry of the AMAP crystal blocks. As a consequence, the AMAP lamellae will grow, leading to an expansion of the AMAP spherulites. The crystal blocks width, t, must increases, while $l_{c\ AMAP}$ would decrease. This is evidenced in Figure 10, where both quantities coincide above 60°C, which corresponds to the isometry of the AMAP phase at higher temperatures.

According to the results of Part I,[1] the early state of retrogradation is characterized by $t/L = 1 - X_c^*$

$= X_{cL}$. This expression corresponds to an isometry of the first emerging AM crystal blocks. The anisometry does not develop below $X_c = 50\%$ (shown here). Above $X_c = 50\%$, the increasing formation of hard AP crystalline spherical shells leads to a compression of the pre-existing AMAP spherulites, leading to the anisometry of its crystalline blocks. This peculiarity of starch gives rise to high fractions of crystallinity.

Temperature range D (67–86°C)

The isometry of the crystal blocks of the AMAP spherulite is maintained in this temperature range (Fig. 10). Because of the spherulitic character of the AMAP crystallization, only the thicker crystal blocks prevail at the beginning of the melting process of the AMAP phase. The D range is subdivided into two parts D_1 and D_2.

Up to 75°C (region D_1), the AP sphere shell semicrystalline superstructure melts up (Fig. 4). At 67°C, the L_{AP} value still reaches with ~14 nm the experimental value of L and that of L_{AMAP} (Fig. 6). This is equivalent to a large distance within between thin crystal shells (same result for the structure of pure crystallized AP[9]). Further melting yields a bursting of the weakened AP shells; the quantity $X_S X_L$ now decreases below 1. When $X_S X_L$ reaches the value $1 - V_{AP} = 0.62$, all free semicrystalline AP grains are molten. This is confirmed by the data of Figure 4 showing that only the AMAP crystalline modification is left ($X_c = 40\%$). Figure 11 confirms that the decrease of $X_S X_L$ (X_c) corresponds to the master curve proposed in Ref. [1]. The range D_1 (67–75°C) is thus characterized by the successive melting (until collapse) of single AP grains.

In the region D_2 (75–86°C), only the AMAP lamellae characterize the long period. Owing to the steep decrease of the total crystallinity, short before the maximum melting point is reached (attributed to melting of AM), it seems reasonable to correlate the linear region before (Fig. 2) to successive melting processes of single AP lamellae within the AMAP spherulite.

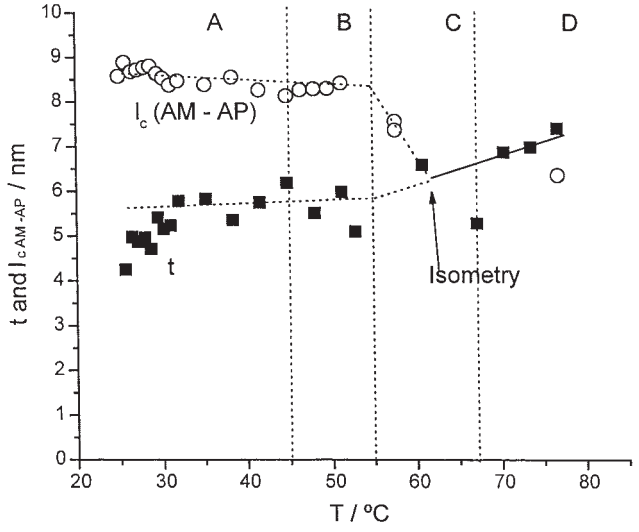

Figure 10 Comparison of $l_{C\ AMAP}$ and t values (from Figs. 7 and 3).

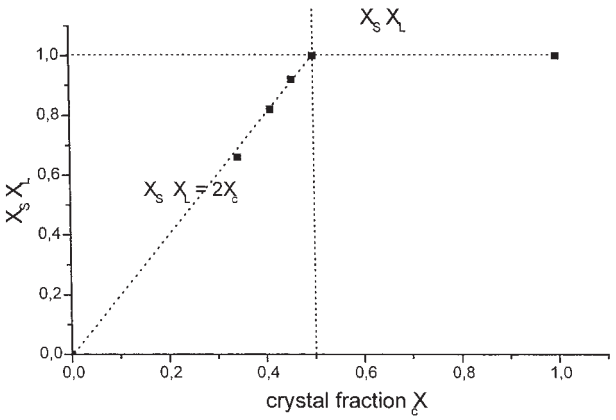

Figure 11 Fraction of semicrystalline material $X_S X_L$ as function of the total crystallinity. Amorphous potato starch crystallized for 20 days in humid atmosphere.

CONCLUSIONS

1. During storage of amorphous potato starch at room temperature in a humid atmosphere, the material attracts water and is converted into a gel. The gel exhibits a high crystallinity level of 65%.
2. Crystalline superstructures depend on the AP molecules, which control the long-range order owing to their large dimensions. One may distinguish between two types of long range order:
   i. A spherulitic order of straight, radial outgoing lamellae from the center of the AP molecule. These lamellae consist either of AM or AP (AMAP crystallization).
   ii. A nanostructure known for pure AP consisting of concentric crystalline sphere shells, separated by amorphous interlayers (AP crystallization).
3. The AMAP crystallization contains the better crystallizing (less branched) AP molecules. The AMAP spherulite is capable to contract, while the semicrystalline grains of free AP molecules, formed at a later stage, need space. This is realized by an increase of crystal thickness and a decrease of the width of the crystalline blocks. This anisotropy of the AMAP crystalline blocks yields an increase of the overall fraction of crystallinity.
4. The AP-(shells)-crystallization contains the more strongly branched AP molecules. Consequently, it originates in regions free of AM. The crystalline

blocks within the AP shell crystals are isometric and smaller than those of AMAP. The existence of the two crystal types implies an inhomogeneity of the AM network within injection-molded potato starch.
5. The AP-crystallization contributes to ~25% to the total crystal fraction, corresponding to 38 vol %, while the AMAP crystallinity amounts to 40%, corresponding to 62% of the total volume.
6. The maximum melt temperature of the AP crystallites is 75°C, the AMAP crystallization is maintained up to 86°C, the most temperature-stable component of both being the pure AM crystals. The anisometry of the AMAP disappears, when the total crystallinity loses its percolation (X_c = 50% at 60°C).

One of us (RKB) gratefully acknowledges the Secretaría de Estado de Universidades e Investigación, MEC, and the "European Social Fund" for the award of a Sabbatical Grant (SAB2003–0131). RKB also thanks the DFG (Deutsche Forschungsgemeinschaft) for the support of this work. The SAXS and WAXS data discussed in this work were derived from measurements carried out at HASYLAB, DESY, Hamburg, under project II-04–029 EC. We thank Arburg Company in Lossburg, Germany, for the kind supply of the injection-molding machine used.

References

1. Bayer, R. K.; Baltá-Calleja, F. J. Int J Polym Mater, to appear.
2. Ziegler, G. R.; Creek, J. A.; Runt, J. Biomacromolecules 2005, 6, 1547.
3. Bayer, R. K.; Dietrich, F.; Lindemann, S.; Ania, F., in preparation.
4. Aberle, T.; Burchard, W. Starch-Stärke 1997, 49, 215.
5. Bayer, R. K.; Zachmann, H. G.; Baltá-Calleja, F. J.; Umbach, H. Polym Eng Sci 1989, 29, 188.
6. Bayer, R. K.; Cagiao, M. E.; Baltá-Calleja, F. J. J Appl Polym Sci, to appear.
7. Bayer, R. K.; Lindemann, S.; Dunkel, M.; Cagiao, M. E.; Ania, F. J Macromol Sci Phys 2001, 40, 733.
8. Cagiao, M. E.; Bayer, R. K.; Rueda, D. R.; Baltá-Calleja, F. J. J Appl Polym Sci 2003, 88, 17.
9. Bayer, R. K.; Baltá-Calleja, F. J. J Appl Polym Sci, to appear.
10. Vandeputte, G. E.; Vermeylen, R.; Geeroms, J.; Delcour, J. A. J Cereal Sci 2003, 38, 61.
11. Bayer, R. K.; Abdelbaghi, M.; Ania, F, in preparation.